

# Migration of sodium and lithium interstitials in anatase TiO<sub>2</sub>

Kordatos, A, Kelaidis, N & Chroneos, A

Author post-print (accepted) deposited by Coventry University's Repository

**Original citation & hyperlink:**

Kordatos, A, Kelaidis, N & Chroneos, A 2018, 'Migration of sodium and lithium interstitials in anatase TiO<sub>2</sub>' *Solid State Ionics*, vol 315, pp. 40-43

<https://dx.doi.org/10.1016/j.ssi.2017.12.003>

DOI 10.1016/j.ssi.2017.12.003

ISSN 0950-7051

ESSN 1872-7409

Publisher: Elsevier

**NOTICE:** this is the author's version of a work that was accepted for publication in *Solid State Ionics*. Changes resulting from the publishing process, such as peer review, editing, corrections, structural formatting, and other quality control mechanisms may not be reflected in this document. Changes may have been made to this work since it was submitted for publication. A definitive version was subsequently published in *Solid State Ionics*, [315, (2017)] DOI: 10.1016/j.ssi.2017.12.003

© 2017, Elsevier. Licensed under the Creative Commons Attribution-NonCommercial-NoDerivatives 4.0 International

<http://creativecommons.org/licenses/by-nc-nd/4.0/>

Copyright © and Moral Rights are retained by the author(s) and/ or other copyright owners. A copy can be downloaded for personal non-commercial research or study, without prior permission or charge. This item cannot be reproduced or quoted extensively from without first obtaining permission in writing from the copyright holder(s). The content must not be changed in any way or sold commercially in any format or medium without the formal permission of the copyright holders.

This document is the author's post-print version, incorporating any revisions agreed during the peer-review process. Some differences between the published version and this version may remain and you are advised to consult the published version if you wish to cite from it.

# Migration of sodium and lithium interstitials in anatase TiO<sub>2</sub>

A. Kordatos<sup>1</sup>, N. Kelaidis<sup>1</sup> and A. Chroneos,<sup>1,2</sup>

<sup>1</sup>*Faculty of Engineering, Environment and Computing, Coventry University, Priory Street,  
Coventry CV1 5FB, United Kingdom*

<sup>2</sup>*Department of Materials, Imperial College, London SW7 2AZ, United Kingdom*

## Abstract

Titanium oxide and in particular anatase is an important material due to its high chemical stability and photocatalytic properties, with the drawback that its large band gap constrains its photocatalytic activity to only a small portion of the solar spectrum. Recently, titanium oxide has been doped with lithium and sodium to consider its potential application in Li-ion and Na-ion batteries, respectively. In the present investigation, we employ density functional theory to study the structure, electronic properties and migration of lithium and sodium interstitials in anatase as these can be important for battery applications. It is shown that the introduction of lithium and sodium interstitials results in energy levels into the band gap. The migration energy barriers of lithium and sodium interstitials are 0.32 eV and 0.56 eV respectively.

## 1. Introduction

The investigation by Fujishima and Honda<sup>1</sup> more than 45 years ago has motivated the community to systematically consider titanium oxide ( $\text{TiO}_2$ ) and other similar metal oxides due to their interesting catalytic activity, high chemical stability and long carrier lifetime of photo-generated electrons.<sup>1-7</sup> Anatase is the  $\text{TiO}_2$  polymorph with the highest photocatalytic activity but it is plagued by its large band gap (3.2 eV) that in essence constrains its activity to the ultraviolet range (i.e. about 5% of the solar spectrum).<sup>4</sup> For photocatalysis,  $\text{TiO}_2$  should have a band gap of about 2 eV whereas the positions of the band edges should be compatible with the redox potential of water.<sup>8</sup> In that respect, nitrogen (N) doping can be employed to decrease the band gap and enhance the visible light response.<sup>9</sup>

Diffusion of lithium (Li) and sodium (Na) in oxides is technologically important to realize Li-ion batteries and more recently Na-ion batteries.<sup>10</sup> Na is considered by the community as a promising alternative as it is abundant and less expensive compared to Li, however, it is a larger atom and typically requires more open host structures to achieve the desired ionic diffusivity.<sup>10,11</sup> Previous studies have determined that  $\text{TiO}_2$  is an important candidate anode material for Li-ion batteries, as it is low cost, environmentally friendly, structurally and electrically stable.<sup>12</sup> The potential of  $\text{TiO}_2$  for Na-ion batteries has been recently discussed.<sup>13</sup>

Atomistic simulation can provide an understanding complementary to experiment of the ion diffusion pathways and the relative energetics of different possible diffusion mechanisms and species at the atomic level. The relative energetics of Li and Na in  $\text{TiO}_2$  are important when considering this system as an anode in batteries. In the present study we use density functional theory (DFT) calculations to investigate Li and Na doping in anatase  $\text{TiO}_2$ . In particular we consider the structure, density of states (DOS) and migration energies of Li and Na interstitials.

## 2. Methodology

The plane wave DFT code CASTEP<sup>14,15</sup> was used. The exchange and correlation interactions were modelled using the corrected density functional of Perdew, Burke and Ernzerhof (PBE)<sup>16</sup> in the generalized gradient approximation (GGA), and with ultrasoft pseudopotentials.<sup>17</sup> The calculations were performed on 108-atomic site supercells under constant pressure conditions, with kinetic energy cut-off of the plane wave basis set to 480 eV and the Monkhorst-Pack (MP)<sup>18</sup> k-point grid being 2 x 2 x 3. Note that a dopant atom represents in the present cell a 0.9% dopant concentration. The correlation effects of localized electrons were considered using onsite Coulomb repulsions of 8.2 eV for the Ti 3d orbitals.<sup>19</sup> For the DOS calculations, a denser mesh of 7 x 7 x 7 k-points was applied. Migration energy barriers were predicted using the linear synchronous transition (LST) and/or quadratic synchronous transition (QST) as implemented in CASTEP.<sup>20</sup>

## 3. Results and Discussion

We have considered anatase (tetragonal with space groups I4/amd) as it is a polymorph of TiO<sub>2</sub> that is being considered for battery applications and additionally has superior photocatalytic properties.<sup>21-24</sup> The calculated lattice parameters of anatase ( $a = 3.806$  Å and  $c = 9.724$  Å) are in very good agreement with neutron diffraction results<sup>23</sup> and previous DFT results.<sup>24,25</sup>

The structure of the anatase unit cell and the minimum energy Li<sub>i</sub> and Na<sub>i</sub> defects in anatase is reported in Fig. 1. These were derived using constant pressure calculations with the host oxide being allowed to relax after the interstitial atom insertion. The minimum energy interstitial sites are the distorted octahedral and not the tetrahedral sites in agreement with previous DFT studies.<sup>26</sup> The distances to the nearest oxygen atoms reveal that Li<sub>i</sub> and Na<sub>i</sub>

defects reside 1.90 Å and 2.10-2.16 Å respectively from the nearest oxygen atom. Figure 1(b) and (c) also reveals that the  $\text{Li}_i$  and  $\text{Na}_i$  defects relax differently as it would be expected by two ions of different size (note that the IV coordination ionic radii of Li and Na are 0.59 Å and 0.99 Å, respectively).

In Fig. 2(a) the DOS of the perfect supercell is shown whereas in Fig. 2(b) and 2(c) we can see the effect of the  $\text{Li}_i$  and  $\text{Na}_i$  defects on the DOS of the supercell.  $\text{Li}_i$  introduces an energy level in the band gap at approximately 2 eV along with a band tail extending 0.26 eV into the valence band. A similar deep level is introduced in the case of  $\text{Na}_i$ , at approximately 1.9 eV above the valence band edge, along with a band tail, which protrudes 0.16 eV into the bandgap. Although it has been reported that the LDA and GGA functionals fail to correctly reproduce the electronic properties of the material even with the inclusion of the Hubbard term, the present DOS are in agreement with previous work that makes use of the sX functional to calculate the impact of  $\text{Li}_i$ .<sup>26</sup> Therefore, in both cases the dopants ( $\text{Li}_i$  and  $\text{Na}_i$ ) introduce deep levels into the bandgap. Even though the leading conduction mechanism is ionic diffusion, the effect of the deep levels have to be taken into consideration when designing an energy application (batteries).

Figure 3 represents the diffusion mechanisms of the  $\text{Li}_i$  and  $\text{Na}_i$  in anatase. For  $\text{Li}_i$  the minimum energy migration path is along the b – axis (refer to Fig. 3(a)) with a migration energy barrier of 0.32 eV (the distance is 3.78 Å). In this mechanism the ion travels below the intermediate oxygen atom that interferes between the initial and final position. As expected, we observe that the initial and final positions of the ions are the most stable interstitial positions in the crystal. For  $\text{Na}_i$  the mechanism is very similar to  $\text{Li}_i$  but with a higher migration energy (0.56 eV). Typically the lower migration energy pathways take advantage of large channels (here the b-axis channel), whereas it was previously proposed that the larger  $\text{Li}_i$ -Ti (or  $\text{Na}_i$ -Ti) atomic distance at the saddle point can be linked to a lower migration

energy barrier.<sup>27</sup> This is because Li diffusion is accelerated by the reduction of the electrostatic  $\text{Li}_i\text{-Ti}$  (or  $\text{Na}_i\text{-Ti}$ ) repulsion. As it can be observed from Table 1 the present results are consistent with lowest energy migration energy being the one that has the larger  $\text{Li}_i\text{-Ti}$  (or  $\text{Na}_i\text{-Ti}$ ) distance.

Considering the migration mechanism along the other directions we examined the movement of the interstitials to several nearest positions and report some characteristic low energy mechanisms (refer to Fig. 3(b) – (d) and Table 1). All these have higher migration energy barriers as compared to the mechanism represented in Fig. 3(a). In Fig. 3(b) the  $\text{Li}_i$  ion diffusion is characterized by a migration energy barrier of 0.58 eV for  $\text{Li}_i$  and 0.78 eV for  $\text{Na}_i$  (distance of 5.45 Å). The migration energy barriers for  $\text{Na}_i$  are higher by as compared to  $\text{Li}_i$ . Therefore, the mechanism along the b-axis (refer to Fig. 3(a)) is the dominant mechanism, nevertheless at higher temperatures the mechanisms of higher energy may also lead to some limited diffusion along other directions.

Finally, experimental work will be required to determine the diffusivities (secondary ion mass spectrometry) and the influence of temperature and processing conditions. It should also be anticipated that the concentration of  $\text{Li}_i$  and  $\text{Na}_i$  may impact the migration energy barriers as it has been previously demonstrated in  $\text{TiO}_2$  and other fast diffusing oxides.<sup>28-30</sup> In particular, in  $\text{TiO}_2$  the increased Li concentration enhances the Li–Li repulsion hindering in turn diffusion.<sup>29</sup> In addition, thermodynamic modelling can also be important to calculate defect parameters and can act synergistically with DFT and experiment.<sup>31-35</sup>

#### 4. Conclusions

In the present study, DFT calculations were used to investigate  $\text{Li}_i$  and  $\text{Na}_i$  diffusion in anatase. It is shown that the minimum energy  $\text{Li}_i$  and  $\text{Na}_i$  defects reside in similar distorted octahedral sites. The  $\text{Na}_i$  defects are larger and distort the lattice more significantly as is

reflected by the oxygen-defect distances. The DOS reveal that both  $\text{Li}_i$  and  $\text{Na}_i$  defects introduce deep levels into the band gap. The preferential diffusion mechanism is along the  $b$  – axis for both  $\text{Li}_i$  and  $\text{Na}_i$  defects with the migration energy barrier for  $\text{Li}_i$  being 0.24 eV lower as compared to  $\text{Na}_i$ .

### **Acknowledgements**

A.K. is grateful for funding from the Faculty of Engineering, Environment and Computing of Coventry University. N.K. and A.C. are grateful for funding from the Lloyd's Register Foundation, a charitable foundation helping to protect life and property by supporting engineering-related education, public engagement and the application of research

## References

- <sup>1</sup>A. Fujishima and K. Honda, *Nature* **238**, 5358 (1972).
- <sup>2</sup>S. U. M. Khan, M. Al-Shahry, and W. B. Ingler, *Science* **297**, 2243 (2002).
- <sup>3</sup>H. G. Yang, C. H. Sun, S. Z. Qiao, J. Zou, G. Liu, S. C. Smith, H. M. Cheng, and G. Q. Lu, *Nature* **453**, 638 (2008).
- <sup>4</sup>Y. Gai, J. Li, S. -S. Li, J. -B., Xia, and S. -H. Wei, *Phys. Rev. Lett.* **102**, 036402 (2009).
- <sup>5</sup>M. Vasilopoulou, D. G. Georgiadou, A. Soultati, N. Boukos, S. gardelis, L. C. Palilis, M. Fakis, G. Skoulatakis, S. Kennou, M. Botzakaki, S. Georga, C. A. Krontiras, F. Auras, D. Fattakhova-Rohlfing, T. Bein, T. A. Papadopoulos, D. Davazoglou, and P. Argitis, *Adv. Energy Mater.* **4**, 1400214 (2014).
- <sup>6</sup>K. Sivula and R. van de Krol, *Nat. Mater. Rev.* **1**, 15010 (2016).
- <sup>7</sup>J. J. Zhu, M. Vasilopoulou, D. Davazoglou, S. Kennou, A. Chroneos, and U. Schwingenschlögl, *Sci. Rep.* **7**, 40882 (2017).
- <sup>8</sup>O. Khaselev and J. A. Turner, *Science* **280**, 425 (1998).
- <sup>9</sup>X. Chen, L. Liu, P. Y. Yu, and S. S. Mao, *Science* **331**, 746 (2011).
- <sup>10</sup>D. Su, S. Dou, and G. Wan, *Chem. Mater.* **27**, 6022 (2015).
- <sup>11</sup>J.-Y. Hwang, S.-T. Myungb and Y.-K. Sun, *Chem. Soc. Rev.* **46**, 3529 (2017).
- <sup>12</sup>J. Wei, J. X. Liu, Y. C. Dang, K. Xu, and Y. Zhu, *Adv. Mater. Res.* **750**, 301 (2013).
- <sup>13</sup>H. Xiong, M. D. Slater, M. Balasubramanian, C. S. Johnson, and T. Rajh, *J. Phys. Chem. Lett.* **2**, 2560 (2011).
- <sup>14</sup>M. C. Payne, M. P. Teter, D. C. Allan, T. A. Arias, and J. D. Joannopoulos, *Rev. Mod. Phys.* **64**, 1045 (1992).
- <sup>15</sup>M. D. Segall, P. J. D. Lindan, M. J. Probert, C. J. Pickard, P. J. Hasnip, S. J. Clark, and M. C. Payne, *J. Phys. Condens. Matter* **14**, 2717 (2002).
- <sup>16</sup>J. Perdew, K. Burke, and M. Ernzerhof, *Phys. Rev. Lett.* **77**, 3865 (1996).
- <sup>17</sup>D. Vanderbilt, *Phys. Rev. B* **41**, 7892 (1990).
- <sup>18</sup>H. J. Monkhorst and J. D. Pack, *Phys. Rev. B* **13**, 5188 (1976).
- <sup>19</sup>E. M. Kiarrii, K. K. Govender, P. G. Ndungu, and P. P. Govender, *Chem. Phys. Lett.* **678**, 167 (2017).



- <sup>20</sup>N. Govind, M. Petersen, G. Fitzgerald, D. King-Smith, and J. Andzelm, *Comput. Mater. Sci.* **28**, 250 (2003).
- <sup>21</sup>M. Xu, Y. Gao, E. M. Moreno, M. Kunst, M. Muhler, Y. Wang, H. Idriss, and C. Wöll, *Phys. Rev. Lett.* **106**, 138302 (2011).
- <sup>22</sup>T. Luttrell, S. Halpegamage, J. Tao, A. Kramer, E. Sutter, and M. Batzill, *Sci. Rep.* **4**, 4043 (2014).
- <sup>23</sup>J. K. Burdett, T. Hughbanks, G. J. Miller, J. W. Richardson, and J. V. Smith, *J. Am. Chem. Soc.* **109**, 3639 (1987).
- <sup>24</sup>J. Muscat, V. Swamy, and N. W. Harrison, *Phys. Rev. B* **65**, 224112 (2002).
- <sup>25</sup>S. Tosoni, O. Lamiel-Garci, D. F. Hevia, J. S. Doña, and F. Illas, *J. Phys. Chem. C* **116**, 12738 (2012).
- <sup>26</sup>J. A. Dawson and J. Robertson, *J. Phys. Chem. C* **120**, 22910 (2016).
- <sup>27</sup>C. Arrouvel, S. C. Parker, and M. S. Islam, *Chem. Mater.* **21**, 4778 (2009).
- <sup>28</sup>D. Parfitt, A. Chroneos, A. Tarancon, and J. A. Kilner, *J. Mater. Chem.* **21**, 2183 (2011).
- <sup>29</sup>H. Yildirim, J. P. Greeley, and S. K. R. S. Sankaranarayanan, *Phys. Chem. Chem. Phys.* **14**, 4565 (2012).
- <sup>30</sup>E. E. Jay, M. J. D. Rushton, A. Chroneos, R. W. Grimes, and J. A. Kilner, *Phys. Chem. Chem. Phys.* **17**, 178 (2015).
- <sup>31</sup>P. Varotsos, *J. Appl. Phys.* **101**, 123503 (2007).
- <sup>32</sup>A. Chroneos and R. V. Vovk, *Solid State Ionics* **274**, 1 (2015)
- <sup>33</sup>M. W. D. Cooper, R. W. Grimes, M. E. Fitzpatrick and A. Chroneos, *Solid State Ionics* **282**, 26 (2015)
- <sup>34</sup>N. V. Sarlis, E. S. Skordas, *J. Phys. Chem. A*, **120**, 1601 (2016).
- <sup>35</sup>A. Chroneos, *Appl. Phys. Rev.* **3**, 041304 (2016).

**Table 1.** The migration energy barriers (ME) and the distances of interstitial atoms to the nearest Ti atom at the saddle point. The numbering of the defect mechanisms corresponds to Fig. 3.

Mechanism	Li <sub>i</sub> ME / eV	Na <sub>i</sub> ME / eV	Li <sub>i</sub> -Ti / Å	Na <sub>i</sub> -Ti / Å
3a	0.32	0.56	2.83	2.83
3b	0.58	0.78	2.57	2.79
3c	0.75	0.81	2.55	2.60
3d	0.74	0.75	2.55	2.57

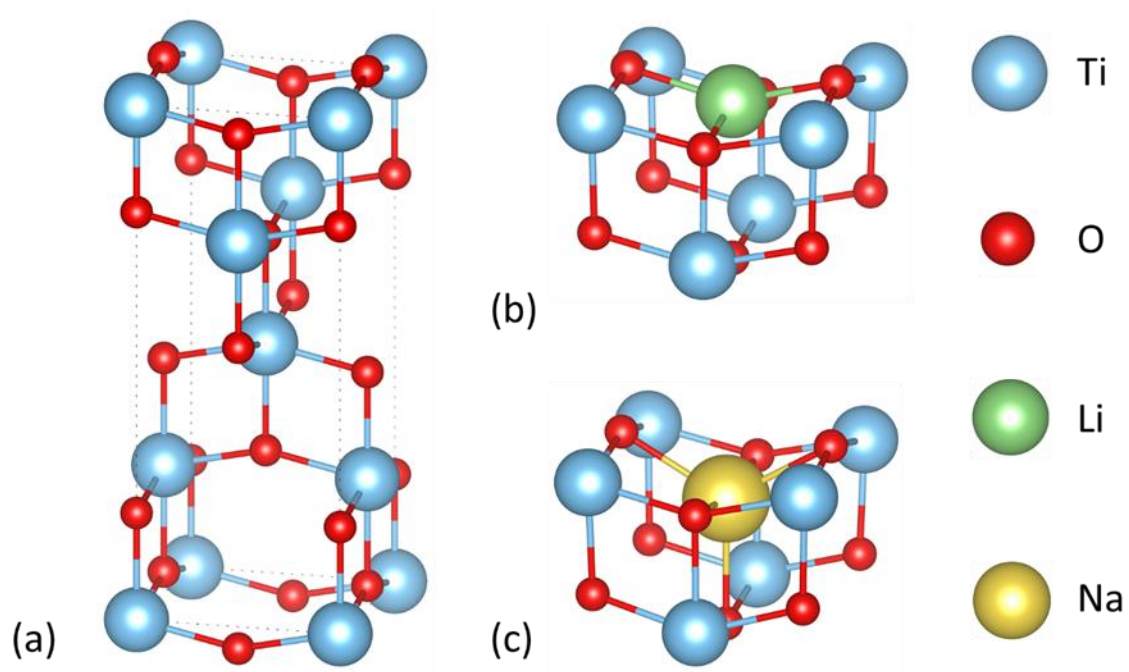
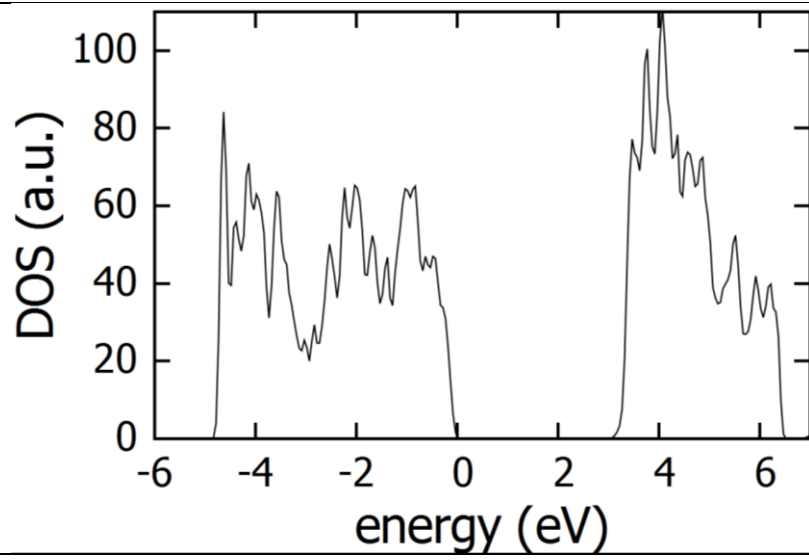
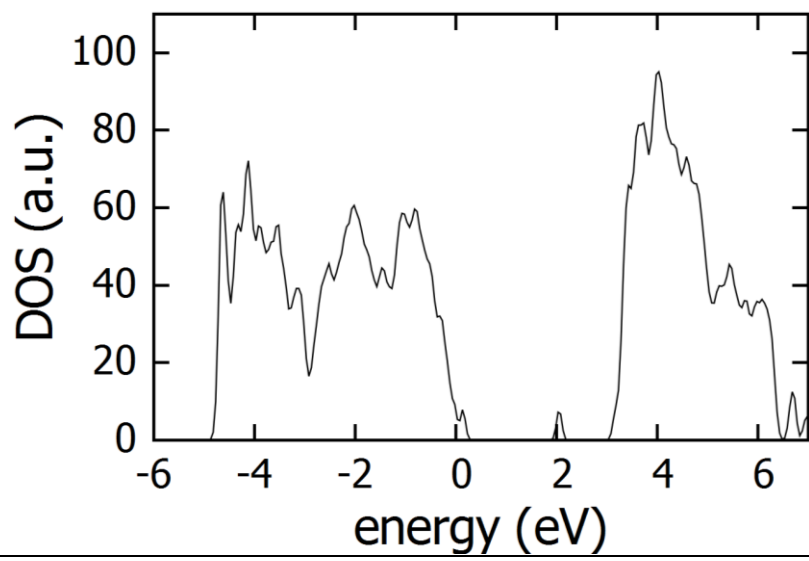


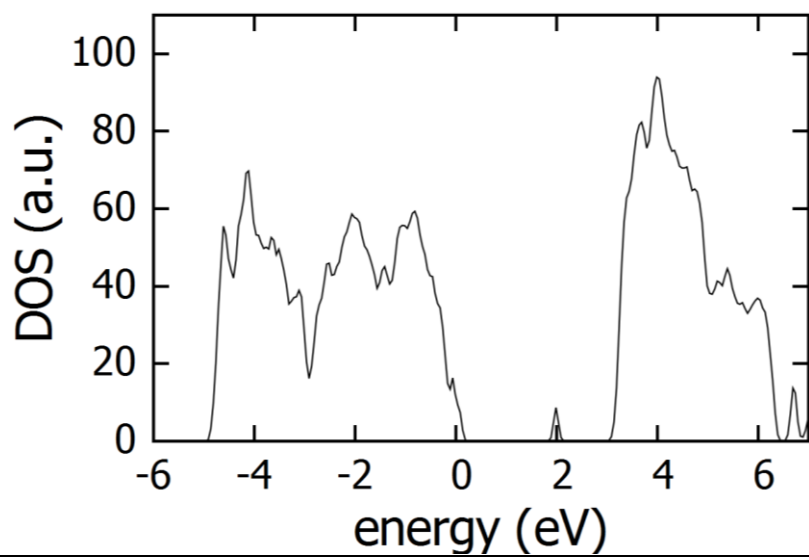
**Figure 1.** The structure of (a) an anatase unit cell and the minimum energy (b) lithium and (c) sodium interstitial defects.



(a)



(b)



(c)

**Figure 2.** Densities of states of (a) the undoped anatase supercell and defective supercells containing (b)  $\text{Li}_i$  and (c)  $\text{Na}_i$ .

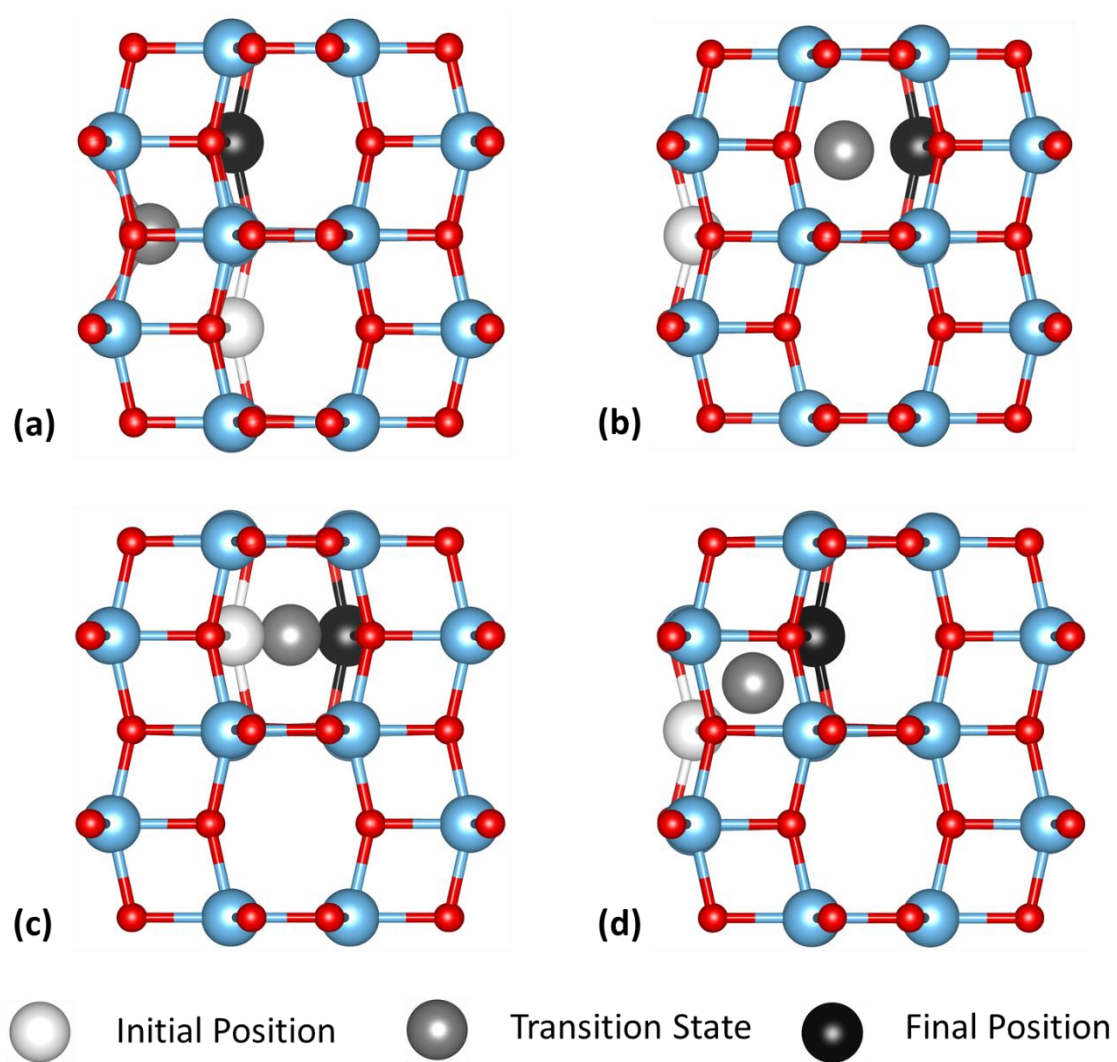


**Figure 3.** (a) –(d) the diffusion mechanisms of  $\text{Li}_i$  and  $\text{Na}_i$  in anatase.